Ciprofloxacin interactions with bacterial protein OmpF: Modelling of FRET from a multi-tryptophan protein trimer

Fábio Fernandes [a], Patrícia Neves [b], Paula Gameiro [b], Luís M.S. Loura [c], Manuel Prieto [a,*]

[a] *Centro de Química-Física Molecular, Instituto Superior Técnico, Lisbon, Portugal*
[b] *Requimte, Departamento de Química, Faculdade de Ciências, Porto, Portugal*
[c] *Faculdade de Farmácia, Universidade de Coimbra, Coimbra, Portugal*

Abstract

The outer membrane protein F (OmpF) is known to play an important role in the uptake of fluoroquinolone antibiotics by bacteria. In this study, the degree of binding of the fluoroquinolone antibiotic ciprofloxacin to OmpF in a lipid membrane environment is quantified using a methodology based on Förster resonance energy transfer (FRET). Analysis of the fluorescence quenching of OmpF is complex as each OmpF monomer presents two tryptophans at different positions, thus sensing two different distributions of acceptors in the bilayer plane. Specific FRET formalisms were derived accounting for the different energy transfer contributions to quenching of each type of tryptophan of OmpF, allowing the recovery of upper and lower boundaries for the ciprofloxacin-OmpF binding constant (K_B). log (K_B) was found to lie in the range 3.15–3.62 or 3.58–4.00 depending on the location for the ciprofloxacin binding site assumed in the FRET modelling, closer to the centre or to the periphery of the OmpF trimer, respectively. This methodology is suitable for the analysis of FRET data obtained with similar protein systems and can be readily adapted to different geometries.
© 2007 Elsevier B.V. All rights reserved.

Keywords: Fluorescence; Fluoroquinolones; Porin; Membrane protein; Membrane model system

1. Introduction

Quinolones are broad-spectrum antibacterial agents which mechanism of action is the inhibition of DNA gyrase and DNA topoisomerase IV enzymes that control DNA topology and are vital for bacterial replication [1–3]. Access to the target site is a major determinant of antibacterial activity, with the outer membrane being the major permeability barrier in Gram negative bacteria [1]. In fact, one of the mechanisms of resistance developed by the bacterial cell is the process of making more difficult the access of quinolones to their target of action, by either not expressing or expressing structurally changed outer membrane porins [3,4]. One of those porins, which microbiology studies related to the permeation of some quinolones through the outer membrane, is OmpF [1,3–6]. Indeed, porin-deficient mutants of *Escherichia coli* are resistant to fluoroquinolones, although the role of OmpF, either as a channel or as an enabler of quinolone diffusion at the OmpF/lipid interface, has not yet been elucidated. The relative importance, and the different areas of contact of each quinolone with OmpF, is a subject of great importance in the context of developing new molecules with less resistance problems.

OmpF is a trimer within the membrane and it contains just two tryptophan residues per monomer (Fig. 1), Trp^{214} at the lipid protein interface and Trp^{61} at the trimer interface [7]. The protein shows a maximum of emission at relatively low wavelengths, which suggests that both tryptophans are in hydrophobic environments. This is confirmed by experiments involving OmpF mutants [7], which lack one or both Trps.
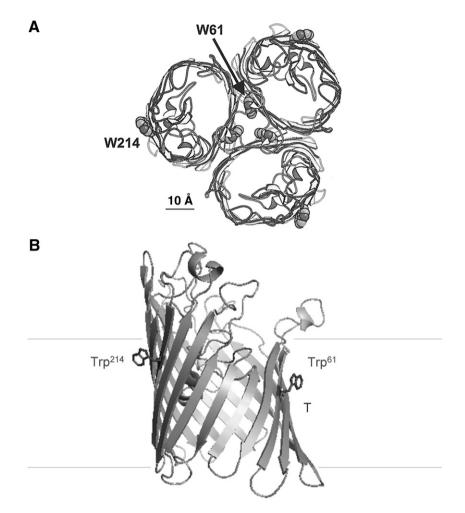
Fig. 1. The structure of the OmpF trimer. The positions of the two Trp residues (Trp^{214} and Trp^{61}) in each monomer are shown. Views of OmpF organization: top (A) (8) (Reproduced by permission of Biophysical Journal) and perpendicular to membrane axis (B). Trimer interface in (B) is assigned by T. The image was draw with PYMOL (DeLano Scientific, San Carlos, CA, http://pymol.sourceforge.net) using PDB coordinates 1OMF1 [22].

Ciprofloxacin (CP) (Fig. 2) is a 6-fluoroquinolone antibiotic currently under clinical use for which many resistances have been reported in a large number of microbial species. The aim of the present study was to investigate the role of OmpF as a major pathway for CP entry through the outer membrane into the bacterial cell by analyzing the alteration of OmpF fluorescence in presence of increasing concentration of CP.

In this way, the extent of Förster resonance energy transfer (FRET) between OmpF and CP was measured, which associated with a rational modelling of the distribution of donor and acceptors in the bilayer allowed us to quantify the extent of binding between the protein and the antibiotic. The FRET modelling presented here is also suitable for application to systems with different geometries, and the new FRET formalisms derived can be readily adapted to the analysis of FRET data obtained with other large membrane proteins presenting donor fluorophores in the protein–lipid interface.

Our study assumes significance in the overall context of the increasing problem of bacterial resistance to the antibiotics currently in use, and the consequent need of understanding the processes involved, in order to create new molecules with increased antibacterial activity and less resistance problems.

2. Materials and methods

Ciprofloxacin (CP) was a gift from Bayer (Leverkusen, Germany). *N*-(2-hydroxyethyl) piperazine-*N′*-ethanesulfonic acid (HEPES) was from Sigma (Sigma, St. Louis, MO). Octylpolyoxyethylene (oPOE) was from Bachem (Bubendorf, Switzerland) and all other chemicals were from Merck (Darmstadt, Germany). All solutions were prepared with 10 mM HEPES buffer (0.1 M NaCl; pH 7.4). OmpF was purified from *E. coli*, strain BL21 (DE3) Omp8, following published procedures [8]. OmpF concentration was estimated using the bicinchoninic acid protein assay against bovine serum albumin as standard.

All the absorption measurements were carried out with a UNICAM UV-300 spectrophotometer equipped with a constant-temperature cell holder. Spectra were recorded at 37 °C in 1 cm quartz cuvettes in the range 230 to 350 nm. Fluorescence measurements were performed in a Varian spectrofluorimeter, model Cary Eclipse, equipped with a constant-temperature cell holder (Peltier
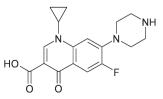

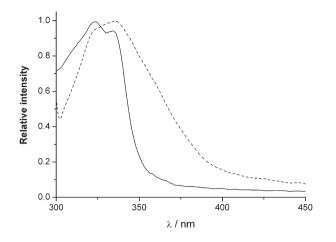Fig. 2. Chemical structure of ciprofloxacin.

Fig. 3. Normalized fluorescence emission spectra of OmpF (---) and absorption spectra of ciprofloxacin (—).

single cell holder). All the spectra were recorded at 37 °C, under constant stirring, with slit widths of excitation and emission of 10 nm.

3. Solutions

All the antibiotic solutions and proteoliposomes suspensions were prepared in 10 mM HEPES buffer (pH 7.4, 0.1 M NaCl).

3.1. Reconstitution of OmpF in DMPC liposomes

As the final purpose for the proteoliposomes was the study of the quinolones interaction with OmpF in a structural perspective, correct orientation of protein insertion was important and best achieved by direct incorporation of OmpF into preformed liposomes [9–12]. Having this into consideration, OmpF proteoliposomes were prepared by direct incorporation into preformed DMPC liposomes, by a well-established methodology [10,13–15]. Briefly, an adequate volume (∼2.6 ml) of DMPC
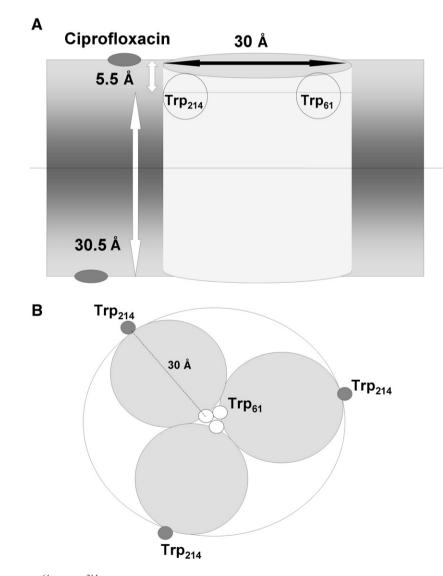

Fig. 4. (A) Positions of donors (Trp[61] and Trp[214]) and acceptors (ciprofloxacin) in the DMPC bilayer. In the simulations, the OmpF monomer is approximated to a cylinder of radius 30 Å (see text). (B) Representation of the OmpF trimer as assumed in the FRET simulations. Trp[61] is located in the trimer interface whereas Trp[214] is located in the periphery of the OmpF trimer.

liposome suspension (∼2.0 mM) in HEPES buffer, prepared according usual procedures [16], is added to OmpF (0.45 mg) in a HEPES buffer solution with 0.4% of oPOE. The lipid/protein mole ratio is always near 1000 and the total volume of the mixture assures a final concentration of oPOE lower than the value of its CMC (0.23%). After an efficient homogenization by gentle stirring, the mixture is incubated 15 min at room temperature followed by 1 h on ice. The detergent is then adsorbed onto SM2 Bio-Beads® from Bio-Rad (Hercules, CA) at a concentration of 0.2 g of Bio-Beads/ml, by gently shaking of the suspension during a period of 3 h. After this time, a second portion of the same amount of Bio-Beads is added and the suspension is again shaken for another 3 h. In the end of this period, proteoliposomes are gently removed by decanting the Bio-Beads. The orientation of OmpF by this reconstitution procedure is considered similar to that observed in the bacterial membranes, based in experimental and molecular dynamics studies [17,18].

As the study to be performed is based on the fluorescence of OmpF, the presence of protein not inserted in the membrane would lead to errors in the final results. The suspension of proteoliposomes was therefore submitted to an ultracentrifugation (80,000×g, 4 °C, 2 h) in order to remove any traces of protein not incorporated. After this procedure the supernatant was rejected and the pellet suspended in HEPES buffer. Protein was quantified in the liposomes and in the supernatant. The percentage of incorporation by this methodology was always higher than 76%. In the final step of the procedure the proteoliposomes are sequentially extruded through 200 and 100 nm polycarbonate membranes from Nucleopore (Kent, WA).

3.2. Quenching of OmpF fluorescence by CP

The fluorescence quenching studies were achieved by successive additions of a constant volume (10 μl) of CP solution (∼296 μM) to the cuvette (final concentration range: 0–38 μM) containing a constant amount of OmpF (∼0.45 μM) incorporated in the liposomes.

Fluorescence spectra were measured with an excitation wavelength of 290 nm. Inner filter effects and dilution of the solution were taken into account.

4. Theoretical modelling

CP quenches OmpF fluorescence through a Förster resonance energy transfer (FRET) mechanism. FRET efficiencies (E) are calculated from the extent of fluorescence emission quenching of the donor induced by the presence of acceptors,

$$E = 1 - \frac{I_{DA}}{I_D} = 1 - \frac{\int_0^\infty i_{DA}(t)\,dt}{\int_0^\infty i_D(t)\,dt} \tag{1}$$

where I_{DA} and I_D are the steady-state fluorescence intensities of the donor in the presence and absence of acceptors respectively. $i_{DA}(t)$ and $i_D(t)$ are the donor fluorescence decays in the presence and absence of acceptors respectively. Although there

is a contribution of static quenching to FRET in OmpF–CP complexes, Eq. (1) still holds since this is taken into account as described below (Eqs. (8)–(12)).

As seen in Fig. 3, CP absorbance overlaps with the OmpF's fluorescence emission spectrum (from both tryptophans 214 and 61), and the overlap integral (J) is calculated as:

$$J = \int f(\lambda) \cdot \varepsilon(\lambda) \cdot \lambda^4 \cdot d\lambda \tag{2}$$

where $f(\lambda)$ is the normalized emission spectrum of the donor and $\varepsilon(\lambda)$ is the absorption spectrum of the acceptor.

The Förster radius (R_0) is given by:

$$R_0 = 0.2108 \cdot (J \cdot \kappa^2 \cdot n^{-4} \cdot \phi_D)^{1/6} \tag{3}$$

where the orientational factor is assumed in the dynamic isotropic regime ($\kappa^2 = 2/3$), the refractive index of the medium is $n = 1.44$, and ϕ_D is the donor quantum yield. The numeric factor in Eq. (3) assumes nm units for the wavelength λ and Å units for R_0.

The Förster radius (R_0) of the Tryptophan(OmpF)–Ciproflaxacin donor–acceptor pair was determined to be 23.3 Å. This is an average value since each of the tryptophans has distinct fluorescence properties and therefore is expected to present different (but, in any case, very similar, probably within 1–2 Å of each other) Förster radii for energy transfer to CP.

Through an analysis of the extent of fluorescence quenching of a donor by the acceptor in a FRET experiment it is possible to calculate a binding constant (K_B) between these two molecules. However, care must be taken when working in solutions where acceptors are highly concentrated, as it is often the case in experiments performed on liposomes. In these cases, when both donors and acceptors partition to the lipid bilayer and interact there, the concentration of acceptors around the donors increases dramatically relatively to a situation where they are both free in solution. FRET can be efficient at distances up to 100 Å depending on the Förster radius of the donor–acceptor pair [19] and therefore, donors in a medium highly concentrated in acceptors, besides being susceptible to fluorescence quenching due to formation of specific donor–acceptor complexes, are also quenched by non-bound, nearby acceptors. Only the first contribution is relevant for the determination of the binding affinity of the donor–acceptor complex, and as the two contributions are not additive (Eq. (4)), formalisms that accurately account for the contribution of non-bound acceptors for the experimentally measured energy transfer efficiencies must be derived, considering the geometrical peculiarities of the studied system. The donor fluorescence decay in the presence of acceptors ($i_{DA}(t)$) is described as:

$$i_{DA}(t) = \gamma \cdot i_D(t) \cdot \rho_{bound}(t) \cdot \rho_{nonbound}(t) \\ + (1 - \gamma) \cdot i_D(t) \cdot \rho_{nonbound}(t) \tag{4}$$

where γ is the fraction of OmpF bound to CP, ρ_{bound} is the FRET contribution from energy transfer to acceptors bound to Ompf, and $\rho_{nonbound}$ is the FRET contribution arising from energy transfer to non-bound acceptors, randomly distributed in different planes (i) from the donors.

4.1. Contribution to FRET of non-bound acceptors

ρ_{nonbound} for a cylindrically symmetric donor geometry is given by [20]:

$$\rho_{\mathrm{nonbound}} = \prod_i \left[\exp\left(-2 \cdot n_2 \cdot \pi \cdot w_i^2 \cdot \int_0^{\frac{w_i}{\sqrt{w_i^2 + R_e^2}}} \frac{1 - \exp(-t \cdot b_i \cdot \alpha^6)}{\alpha^3} \, d\alpha \right) \right] \tag{5}$$

where $b_i = (R_0^2/w_i)^2 \tau_D^{-1/3}$, n_2 is the acceptor density in each bilayer leaflet (number of acceptors per unit area), w_i is the
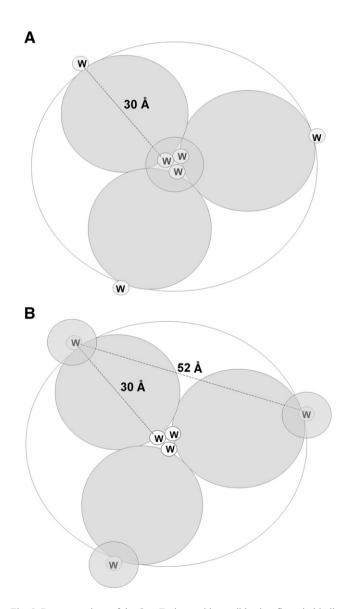

Fig. 5. Representations of the OmpF trimer with possible ciprofloxacin binding sites specified (diagonal filling) for each of chosen binding models. (A) Model I: binding site for ciprofloxacin is located near the trimer interface. Quenching of Trp[61] is complete after antibiotic binding, while the three Trp[214] are at a distance of 30 Å from ciprofloxacin. (B) Model II: binding site for ciprofloxacin is located in the trimer periphery near one of the Trp[214] which is completely quenched after binding. The other Trp[214] are at a distance of 52 Å from the binding site, whereas the three Trp[61] are at a distance of 30 Å.

distance between the plane of the donors and the i-th plane of acceptors and R_e is the donor exclusion radius (which defines the area around the donor from where the acceptors are excluded). In protein–ligand FRET studies the exclusion radius is particularly important if the size of the protein is comparable to the Förster radius of the donor–acceptor pair.

In order to calculate ρ_{nonbound}, a model must be used to describe the positions of the donors and acceptors in the bilayer. OmpF has two clear belts of aromatic residues at the lipid/water interface separated by 25 Å [21]. Both Trps (61 and 214) are located in the same aromatic belt and are assumed to be in the same plane, at 12.5 Å from the center of the bilayer. When incorporated in liposomes, CP is located in the headgroup region of the bilayer [22] and according to Nagle and Tristan-Nagle [23] for DMPC the headgroups average position is 18 Å away from the centre of the bilayer. In the FRET simulations this is considered to be the position of the plane of acceptors and w_1 and w_2 are assumed to be 5.5 Å and 30.5 Å (Fig. 4A). In our formalism we consider that there is no partition of non-bound CP in the bilayer area occupied by the OmpF trimer apart from the specifically bound population of antibiotic molecules.

Trp[61] is located at the trimer interface (Fig. 4B) and the exclusion area for non-bound CP will be significant. R_e (Eq. (5)) of Trp[61] is assumed to be 30 Å which is the approximate diameter of an OmpF monomer in the bilayer plane [24] (Fig. 4B).

On the other hand, Trp[214] is located in the periphery of the OmpF trimer and the distribution of non-bound CP around it will be cylindrically asymmetric. This difference in the distribution of acceptors sensed by the two donors (Trp[214] and Trp[61]) can only be accounted through the use in the FRET simulations of two different ρ_{nonbound} contributions.

For Trp[61] the FRET contribution is simply given by Eq. (5) and setting $i=2$, $w_1=5.5$ Å, $w_2=30.5$ Å and $R_e=30$ Å. In the case of Trp[214] a large section of the bilayer is also occupied by the protein trimer itself and inaccessible to acceptors. However, this placement of the protein around the tryptophan is no longer symmetrical as for Trp[61], and energy transfer must be accounted differently:

$$\rho_{\mathrm{nonbound}'}(t) = \prod_i \left[\exp\left\{ -2\pi n_2 w_i^2 \left[\int_{w_i/\sqrt{w_i^2 + R_d^2}}^{w_i/\sqrt{w_i^2 + R_p^2}} \left\{ 1 - \exp\left[\left(-\frac{t}{\tau_D} \right) \left(\frac{R_0}{w_i} \right)^6 \alpha^6 \right] \right\} f(\alpha) \, d\alpha \right. \right. \right.$$
$$\left. \left. \left. - \int_{w_i/\sqrt{w_i^2 + R_p^2}}^{1} \exp\left[\left(-\frac{t}{\tau_D} \right) \left(\frac{R_0}{w_i} \right)^6 \alpha^6 \right] f(\alpha) \alpha^{-3} \, d\alpha \right] \right\} \right] \tag{6}$$

$\rho_{\mathrm{nonbound}'}$ is therefore the FRET contribution to the decay of a donor located in the surface of a protein of radius R_P due to the presence of acceptors randomly distributed in i different planes (for details on the derivation of this component and on function f(α) see Appendix).

Using Eqs. (1) and (4)–(6), theoretical expectations for FRET efficiencies for a random distribution of acceptors can be estimated.

In the simulations and data analysis of FRET efficiencies it was considered that Trp[61] and Trp[214] contributed equally to the fluorescence intensity of the protein. Also, energy migration among the Trp[61] does not affect the geometry of the problem, and energy

migration between Trp[61] and Trp[214] is a very inefficient process due to the distance (30 Å) between the two residues.

4.2. Contribution to FRET of specifically bound acceptors

To quantify the contribution of specifically bound CP to FRET, it is first necessary to relate the binding constant of this antibiotic and OmpF (K_B) to the factor γ (fraction of OmpF bound to CP) in Eq. (4):

$$\gamma = \left[\frac{(1 + [\text{OmpF}] \cdot K_B + [\text{CP}] \cdot K_B) +}{\sqrt{(1 + [\text{OmpF}] \cdot K_B + [\text{CP}] \cdot K_B)^2 - 4 \cdot K_B^2 \cdot [\text{OmpF}] \cdot [\text{CP}]}} \right] \Big/ 2 \cdot K_B \cdot [\text{OmpF}]_{\text{Total}}$$

(7)

where $[\text{OmpF}]_{\text{Total}}$ and $[\text{OmpF}]$ are the total and unbound concentrations of OmpF, and $[\text{CP}]$ is the concentration of
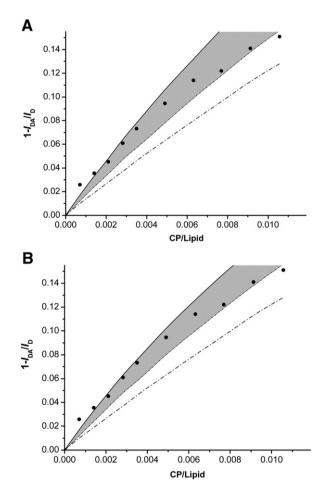
Fig. 6. Extent of energy transfer (Eq. (1)) for the OmpF tryptophan-Ciprofloxacin, donor acceptor FRET pair. Simulation for absence of binding (random distribution of acceptors) (Eqs. (4)–(6)) (·–·–·). (A) A model assuming binding of ciprofloxacin near the trimer interface (Model I) was fitted to the experimental data (Eqs. (4)–(12)). The interval of $3.15 < \log(K_B) < 3.62$ was recovered for the binding constant (grey area). (B) A model assuming binding of ciprofloxacin to the OmpF periphery (Model II) was fitted to the experimental data. The interval of $3.58 < \log(K_B) < 4.00$ was recovered for the binding constant (grey area). The simulations for the upper and lower bounds of K_B are represented in both figures by a solid line (—) and by a dotted line (·····), respectively.

Table 1
Lower and upper limits for the binding constants of CP-OmpF for each of the CP binding sites considered in the analysis

	$\log(K_B)_{\text{(lower limit)}}$	$\log(K_B)_{\text{(upper limit)}}$
Model I [a]	3.15	3.62
Model II [b]	3.58	4.00

[a] CP binding site is assumed to be in close proximity to Trp[61].
[b] CP binding site is assumed to be close to the periphery of the trimer, near Trp[214].

unbound CP. It is assumed that only 1:1 complexes can be formed between OmpF and CP. The 1:1 complex model is supported by data from a previous study [25].

In the event of binding of CP to Ompf, the fluorescence of the several Trps present in one trimer will be quenched differently, as the distances between them and the antibiotic will be also different. Therefore, also for ρ_{bound}, two different contributions for Trp[214] and Trp[61] must be considered.

$$\rho_{\text{bound}} = \rho_{\text{bound}(\text{Trp}^{214})} + \rho_{\text{bound}(\text{Trp}^{61})}$$

(8)

Assuming that at least one of the tryptophans of OmpF is part of a hypothetical CP binding site and subsequently completely quenched, and that no more than one antibiotic molecule can be specifically bound to a OmpF trimer at a given time, two models were devised: (i) the CP binding site is close to the center of the trimer and binding of antibiotic leads to complete quenching of the three Trp[61] (distance of Trp[61] to CP $\ll R_0$) (Fig. 5A); (ii) the binding site is near the protein–lipid interface (Fig. 5B). In the first case (Model I), it is assumed that only the three Trp[214] residues remain fluorescent ($\rho^I_{\text{bound}(\text{Trp}61)} = 0$) and the CP binding site is located at 30 Å (d_1, trimer radius) from them. The contribution to FRET of specifically bound CP is given by:

$$\rho^I_{\text{bound}(\text{Total})}(t) = \rho^I_{\text{bound}(\text{Trp}^{214})}(t) = \exp\left(-\frac{t}{\tau_D} \cdot \left(\frac{R_0}{d_1}\right)^6\right)$$

(9)

where τ_D is the average donor lifetime.

In the case of binding of CP near the surface of the OmpF trimer (Model II) with complete quenching of one Trp[214], the antibiotic molecules will be located at a distance of 30 Å (d_1') from Trp[61] (the centre of mass of the three Trp[61] is located in the centre of the trimer) and 52 Å (d_2) from the other two Trp[214]. As a result, $\rho^{II}_{\text{bound (Trp}^{214})}$ is multiplied by 2/3 and the contributions to FRET of specifically bound CP are given by:

$$\rho^{II}_{\text{bound}(\text{Total})} = \rho^{II}_{\text{bound}(\text{Trp}^{61})}(t) + \frac{2}{3} \cdot \rho^{II}_{\text{bound}(\text{Trp}^{214})}(t)$$

(10)

$$\rho^{II}_{\text{bound}(\text{Trp}^{61})}(t) = \exp\left(-\frac{t}{\tau_D} \cdot \left(\frac{R_0}{d_1'}\right)^6\right)$$

(11)

$$\rho^{II}_{\text{bound}(\text{Trp}^{214})}(t) = \exp\left(-\frac{t}{\tau_D} \cdot \left(\frac{R_0}{d_2}\right)^6\right)$$

(12)

5. Results and discussion

Successive additions of small volumes of a CP solution to OmpF proteoliposomes resulted as expected in a decrease of fluorescence from OmpF (Fig. 6). Using Eqs. (4)–(6) it is possible to compare the theoretical expectation for the efficiencies of energy transfer from the tryptophans of OmpF to unbound CP (randomly distributed) with the data obtained experimentally. Clearly the extent of quenching of the tryptophans cannot be exclusively explained on the basis of energy transfer to unbound CP, and a FRET contribution to specifically associated antibiotic must be considered.

The binding constants that allow for better fits to the data points are different depending on the model for binding that is considered (I or II). In the case of model I, that assumes binding of CP close to the centre of the trimer, quenching is much more effective as the binding site is in the vicinity of three tryptophans (Trp[61]), while for model II only one tryptophan is located near the bound antibiotic. This results in the recovery of larger K_B values for model II than for model I. Upper and lower limits for K_B (that allow respectively for better fits to the data points corresponding to the lower and higher CP concentration ranges) were determined for each model, and are shown in Table 1.

In a previous study, changes in CP absorption spectra were used to estimate a OmpF-CP binding constant and values of log $(K_B)=3.85\pm0.34$ or 4.17 ± 0.03 were obtained depending on the method chosen to analyze the absorption spectra changes after addition of OmpF in a micellar environment [25]. These values fall within or close to the range of K_B obtained by us from the energy transfer data assuming binding of CP to the periphery of OmpF $(3.58<K_B<4.00)$. This agreement with an alternative method can be seen as an indication that the antibiotic binding site is likely to be located away from the centre of the OmpF trimer where FRET would be more efficient and imply a smaller K_B.

6. Conclusions

In the present study, the CP fluoroquinolone is shown to associate with OmpF using FRET methodologies. The high symmetry of the OmpF trimer allowed the analysis of FRET data with formalisms that accounted for the different distributions of acceptors around the two types of tryptophans present in the protein. This methodology is suitable for application in the analysis of FRET data obtained with similar protein systems and can be adapted to different geometries. The new FRET formalisms presented here for a donor in the surface of a cylinder of large radius (with radius comparable to the Förster radius) are expected to be of great assistance in the analysis of FRET data obtained with membrane proteins presenting donor fluorophores in the protein–lipid interface.

The equilibrium constant retrieved for the association event between OmpF and CP assuming binding of the antibiotic in the periphery of the porin is in agreement with a value determined previously by an independent method (in a micellar environment), indicating that the binding site of the antibiotic is likely to be located away from the center of OmpF. Also, the FRET

methodology can be applied in cases where there are no spectral shifts, and its sensitivity is higher as compared to absorption methodologies.

Appendix A. Derivation of the FRET rate between a donor at the outer radius of a cylindrical transmembrane protein to a plane of acceptors distributed around the latter

Fig. A1 shows the geometry relevant to this problem. Our derivation of the FRET rate law begins with the general expression for the average decay for a donor located in the centre of a finite disk with radius R_d, $<\rho(t)>_N$, taking into account all statistical arrangements of the N acceptor molecules located inside the disk [26]:

$$<\rho(t)>_N = \exp(-t/\tau) \cdot \prod_{i=1}^{N} \int_{w}^{\sqrt{w^2+R_d^2}} \exp\left[-\frac{t}{\tau}\left(\frac{R_0}{R_i}\right)^6\right] W(R_i)\mathrm{d}R_i \tag{A1}$$

where $W(R_i)\mathrm{d}R_i$ is the probability of finding acceptor molecule A_i in the ring of inner radius R_i and outer radius $R_i+\mathrm{d}R_i$. The acceptor distribution function is normalized, in the sense that

$$\int_{w}^{\sqrt{w^2+R_d^2}} W(R_i)\mathrm{d}R_i = 1 \tag{A2}$$

We now proceed as previously done by Davenport et al. [20] and Capeta et al. [27] for similar (albeit simpler) geometries. Because all acceptors have the same distribution function, $W(R_i)$
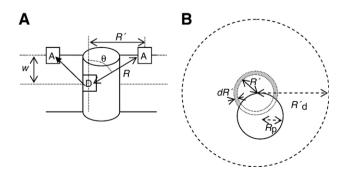

Fig. A1. Schematic side (A) and top (B) views of a lipid bilayer containing a cylindrical membrane protein labelled with a donor fluorophore (D) at its outer radius, capable of FRET to acceptors (A) located in the lipid bilayer, on a plane parallel to the bilayer plane. See text for details.

$dR_i = W(R_j)dR_j =$ simply $W(R)dR$, all integrals in Eq. (A1) are identical, and denoting them by $J(t)$, we can write

$$<\rho(t)>_N = \exp\left(-\frac{t}{\tau_D}\right) \cdot [J(t)]^N \tag{A3}$$

As pointed out by Davenport et al. [20], the probability of finding an acceptor at a distance between R and $R+dR$ to the donor in question, given by $W(R)dR$, is equal to that of finding an acceptor in the ring between R' and $R'+dR'$ in the acceptors plane, given by $W(R')dR'$. The acceptor distribution function, in terms of $R'=R\sin\theta$ (see Fig. A1A), is given by

$$W(R') = \begin{cases} \dfrac{[1 + (2/\pi)\arcsin(R'/2R_p)]R'}{R_d'^2 - R_p^2} & 0<R'<2R_p \\ \dfrac{2R'}{R_d'^2 - R_p^2} & 2R_p<R'<R_d' \end{cases} \tag{A4}$$

Note that, whereas for $R'>2R_p$ (where R_p is the cylindrical protein radius) $W(R')$ is as expected for a uniform distribution of acceptors in a planar disk (only corrected in the denominator for the excluded area resulting from the existence of a protein molecule inside R_d), for $R'<2R_p$ the more complex expression denotes that only a fraction of the region between R' and $R'+dR$ is available to acceptors (the shaded area in Fig. A1B). Insertion of this distribution function in the definition of $J(t)$ (the integral in Eq. (A1)), together with the substitution $\alpha=\cos\theta=w/R$, leads to

$$J(t) = \frac{2w^2}{R_d'^2 - R_p^2} \int_{w/\sqrt{w^2+R_d'^2}}^{1} \exp\left[\left(-\frac{t}{\tau_D}\right)\left(\frac{R_0}{w}\right)^6 \alpha^6\right] f(\alpha)\alpha^{-3}d\alpha \tag{A5}$$

where

$$f(\alpha) = \begin{cases} 1 & \dfrac{w}{\sqrt{w^2+R_d'^2}}<\alpha<\dfrac{w}{\sqrt{w^2+4R_p^2}} \\ \dfrac{1}{2}+\dfrac{1}{\pi}\arcsin\left(\dfrac{w\sqrt{1-\alpha^2}}{2\alpha R_p}\right) & \dfrac{w}{\sqrt{w^2+4R_p^2}}<\alpha<1 \end{cases} \tag{A6}$$

We now rearrange Eq. (A5) into

$$J(t) = \frac{2w^2}{R_d'^2 - R_p^2}\left(\int_{w/\sqrt{w^2+R_d'^2}}^{w/\sqrt{w^2+R_p^2}} \alpha^{-3}d\alpha - \int_{w/\sqrt{w^2+R_d'^2}}^{w/\sqrt{w^2+R_p^2}}\left\{1-\exp\left[\left(-\frac{t}{\tau_D}\right)\left(\frac{R_0}{w}\right)^6\alpha^6\right]f(\alpha)\right\}d\alpha\right.$$

$$\left. + \int_{w/\sqrt{w^2+R_p^2}}^{1}\exp\left[\left(-\frac{t}{\tau_D}\right)\left(\frac{R_0}{w}\right)^6\alpha^6\right]f(\alpha)\alpha^{-3}d\alpha\right) \tag{A7}$$

and denote the integrals on the right hand side of Eq. (A7) by J_1, $J_2(t)$ and $J_3(t)$, according to the order in which they appear in this equation. J_1 is easily calculated, leading to

$$J(t) = 1 - \frac{2w^2}{R_d'^2 - R_p^2}[J_2(t) - J_3(t)] \tag{A8}$$

Being the average concentration of acceptors in the bilayer given by,

$$n_2 = \frac{N}{\pi(R_d'^2 - R_p^2)} \tag{A9}$$

it follows that

$$J(t) = 1 - \frac{2\pi n_2 w^2}{N}[J_2(t) - J_3(t)] \tag{A10}$$

Inserting this expression for $J(t)$ in Eq. (A1), and taking the limit $(N\to\infty, R_d'\to\infty)$, one obtains the macroscopic decay law. The result is,

$$\rho(t) = \exp\{-2\pi n_2 w^2[J_2(t) - J_3(t)]\} \tag{A11}$$

which is equivalent to each of the i items in the product of the right hand side of Eq. (6).

References

[1] J.S. Chapman, N.H. Georgopapadakou, Routes of quinolone permeation in *Escherichia coli*, Antimicrob. Agents Chemother. 32 (1988) 438–442.

[2] E. Pestova, J.J. Millichap, G.A. Noskin, L.R. Peterson, Intracellular targets of moxifloxacin: a comparison with other fluoroquinolones, J. Antimicrob. Chemother. 45 (2000) 583–590.

[3] O.A. Mascaretti, Bacteria versus Antibacterial Agents: An integrated approach, ASM Press, Washington D.C., 2003.

[4] J. Chevalier, M. Malléa, J.-M. Pagès, Comparative aspects of the diffusion of norfloxacin, cefepime and spermine through the F porin channel of *Enterobacter cloacae*, Biochem. J. 348 (2000) 223–227.

[5] L.J.V. Piddock, Y.-F. Jin, V. Ricci, A.E. Asuquo, Quinolone accumulation by *Pseudomonas aeruginosa*, *Staphylococcus aureus* and *Escherichia coli*, J. Antimicrob. Chemother. 43 (1999) 61–70.

[6] K. Hirai, H. Aoyama, T. Irikura, S. Iyobe, S. Mitsuhashi, Differences in susceptibility to quinolones of outer membrane mutants of *Salmonella typhimurium* and *Escherichia coli*, Antimicrob. Agents Chemother. 29 (1986) 535–538.

[7] A.H. O'Keeffe, J.M. East, A.G. Lee, Selectivity in lipid binding to the bacterial outer membrane protein OmpF, Biophys. J. 79 (2000) 2066–2074.

[8] R.M. Gravito, J.P. Rosenbusch, Isolation and crystallization of bacterial porin, Methods Enzymol. 125 (1986) 309–328.

[9] J.-L. Rigaud, B. Pitard, D. Levy, Reconstitution of membrane proteins into liposomes: application to energy transducing membrane proteins, Biochim. Biophys. Acta 123 (1995) 223–246.

[10] J.-L. Rigaud, M.T. Paternostre, A. Bluzat, Mechanisms of membrane protein insertion into liposomes during reconstitution procedures involving the use of detergents. 2. Incorporation of the light-driven proton pump bacteriorhodopsin, Biochemistry 27 (1988) 2677–2688.

[11] P. Richard, J.-L. Rigaud, P. Graber, Reconstitution of CF0F1 into liposomes using a new reconstitution procedure, Eur. J. Biochem. 193 (1990) 921–930.

[12] D. Levy, A. Gulik, A. Bluzat, J-L. Rigaud, Reconstitution of the sarcoplasmic reticulum Ca^{2+}ATPase: mechanisms of membrane protein insertion into liposomes during reconstitution procedures involving the use of detergents, Biochim. Biophys. Acta 1107 (1992) 283–298.

[13] M.T. Paternostre, M. Roux, J.-L. Rigaud, Mechanisms of membrane protein insertion into liposomes during reconstruction procedures involving the use of detergents. Solubilization of large unilamellar liposomes (prepared by reverse-phase evaporation) by Triton X-100, octyl glucoside and sodium cholate, Biochemistry 27 (1988) 2668–2677.

[14] L. Plançon, M. Chami, L. Letellier, Reconstitution of FhuA, an *Escherichia coli* outer membrane protein, into liposomes, J. Biol. Chem. 272 (1997) 16868–16872.

[15] J. Knol, K. Sjollema, B. Poolman, Detergent-mediated reconstitution of membrane proteins, Biochemistry 37 (1998) 16410–16415.

[16] A.D. Bangham, M.M. Standish, J.C. Watkins, Diffusion of univalent ions across the lamellae of swollen phospholipids, J. Mol. Biol. 13 (1965) 238–252.

[17] W. Im, B. Roux, Ions and counterions in a biological channel: a molecular dynamics simulation of OmpF porin from *Escherichia coli* in an explicit membrane with 1 M KCl aqueous salt solution, J. Mol. Biol. 319 (2002) 1177–1197.

[18] E.M. Nestorovich, C. Danelon, M. Winterhalter, S.M. Bezrukov, Designed to penetrate: time-resolved interaction of single antibiotic molecules with bacterial pores, Proc. Natl. Acad. Sci. U. S. A. 99 (2002) 9789–9794.

[19] J.R. Lakowicz, Principles of fluorescence spectroscopy. Chapter 13, 3rd edition, Springer Science, New York, 2006, pp. 443–475.

[20] L. Davenport, R.E. Dale, R.E. Bisby, R.B. Cundall, Transverse location of the fluorescent probe 1,6-diphenyl-1,3,5-hexatriene in model lipid bilayer membrane systems by resonance energy transfer, Biochemistry 24 (1985) 4097–4108.

[21] D.W. Martin, Active unit of solubilized sarcoplasmic reticulum calcium adenosinetriphophatase: an active enzyme centrifugation analysis, Biochemistry 22 (1983) 2276–2282.

[22] J.L. Vazquez, M.T. Montero, S. Merino, O. Domenech, M. Berlanga, M. Vinas, J. Hernandez-Borrel, Location and nature of the surface membrane binding site of ciprofloxacin: a fluorescence study, Langmuir 17 (2001) 1009–1014.

[23] J.F. Nagle, S. Tristam-Nagle, Structure of lipid bilayers, Biochim. Biophys. Acta 1469 (2000) 159–195.

[24] S.W. Cowan, R.M. Garavito, J.N. Jansonius, J.A. Jenkins, R. Karlsson, N. Konig, E.F. Pai, R.A. Pauptit, P.J. Rizkallah, J.P. Rosenbusch, G. Rummel, T. Schimer, The structure of OmpF porin in a tetragonal crystal form, Structure 10 (1995) 1041–1050.

[25] P. Neves, E. Berkane, P. Gameiro, M. Winterhalter, B. de Castro, Interaction between quinolones antibiotics and bacterial outer membrane porin OmpF, Biophys. Chemist. 113 (2005) 123–128.

[26] P.K. Wolber, B.S. Hudson, An analytical solution to the Förster energy transfer problem in two dimensions, Biophys. J. 28 (1979) 197–210.

[27] R.C. Capeta, J.A. Poveda, L.M.S. Loura, Non-uniform membrane probe distribution in resonance energy transfer. Application to protein–lipid selectivity, J. Fluoresc. 16 (2005) 161–172.